



Research article

Emissions from the combustion of torrefied and raw biomass fuels in a domestic heating stove



D. Maxwell, B.A. Gudka, J.M. Jones, A. Williams*

School of Chemical and Process Engineering, University of Leeds, Leeds LS2 9JT, UK

ARTICLE INFO

Keywords:

Torrefied biomass
Combustion
Pollutant
Fixed-bed stove

ABSTRACT

Biomass (pellets, briquettes, logs) are a key contributor to many countries' strategies for decarbonising heat, particularly in domestic applications. The emissions from these small devices can be high and severely impact air quality, but their levels depend on the design, control, abatement and fuel options. This paper is concerned with the last case. A comparative study shows the emissions from a domestic wood stove for three biomass fuels and their torrefied counterparts. The fuels were burned in a multi-fuel stove along with two reload batches creating continuous combustion cycles: the initial cold start data is presented but not included in averaging and calculation of emission factors. Measurements were made using an FTIR instrument for carbon and nitrogen based gaseous emissions, particulates were measured using a smoke meter with micro-quartz filters as well as a size-selective impactor to obtain the particle size distribution. Particulate emissions were significantly reduced from the torrefied fuels and this is thought to be related to their pyrolysis fingerprint, which was investigated by pyrolysis-GC-MS. NO_x was slightly reduced, despite increased fuel-N after torrefaction. In addition, the reduced moisture in the torrefied fuels decreases emissions of CO and CH₄ because of increased time of flaming combustion.

1. Introduction

Biomass utilisation, as with other renewable energy sources, has increased mainly due to global warming concerns. This has been the case at two extremes of scale: large scale electricity generation through to small scale domestic application. In the case of the former, there has been considerable interest in the application of biomass torrefaction in order to improve the properties of wood especially for energy densification, handling properties and ease of grinding [1–6]. The use of torrefied wood can result in the emission of less pollutants than from burning coal and, depending on the conditions sometimes less, than the equivalent wood [7]. Recently concerns have been expressed about the large-scale use of bioenergy resources for electricity generation [8,9] and whilst these may be over emphasised [10–12] there has been a diminishment, although mainly for economic reasons, in the application of torrefaction in this field. Domestic stoves for heating and cooking applications are a large part of the increased use of biomass for bioheat, especially in Europe. Consequently attention has been given to the domestic use of torrefied biomass, where there have been very few studies [13–15], or for the potential use of torrefied biomass in gasification [6,16]. In both of these cases there would be significant benefits in improved energy densification, in fuel handling and overall

combustion emissions.

The combustion of raw wood results in the emission of fine particles which have adverse health effects [17–20], and a major advantage of torrefaction appears to be a reduction of the number of fine particles produced [14,16]. A number of papers have considered the nature and effect of fine particles produced by wood combustion [20–24]. Atiku et al. [25] showed that the pyrolysis of wood formed decomposition products, such as furfural, that reacted in diffusion flames and formed fine carbonaceous particles (ultra-fine particles) that grew in size and agglomerated into 1 to 2.5 μm diameter particles. Further work [26] modelled the mechanism of soot formation. This indicated that certain pyrolysis products, such as eugenol, which is typical of lignin decomposition to substituted propylphenols, are highly sooting since they can contribute to the two main routes in soot formation, HACA (hydrogen abstraction, carbon addition) and via cyclopentadiene formation and reaction. This indicates that the pyrolysis fingerprint of a fuel is a contributing factor to the rate of soot formation during combustion. Studies of the pyrolysis fingerprints of torrefied biomass versus non-torrefied counter parts [27,28] indicate that some of the more sooting components decrease in concentration after torrefaction and this may partly explain the reduction in fine particulate during combustion of torrefied biomass.

* Corresponding author.

E-mail address: a.williams@leeds.ac.uk (A. Williams).<https://doi.org/10.1016/j.fuproc.2019.106266>

Received 12 July 2019; Received in revised form 31 October 2019; Accepted 1 November 2019

Available online 10 November 2019

0378-3820/© 2019 The Authors. Published by Elsevier B.V. This is an open access article under the CC BY license (<http://creativecommons.org/licenses/by/4.0/>).

Table 1
Fuels used in these experiments.

Fuel no	Sample	Source	Shape/dimensions (mm)	Moisture, ar, wt%
1	Norway spruce	Aberdeenshire Scotland	Half split logs; with bark included 140 × 80 × 50	18
2	Torrefied spruce briquettes	Andritz AG, Austria	Circular briquettes 70 × 60 (length × diam.)	4.6
3	Willow logs	RSPB, Idle Valley, Nottinghamshire	1/2 split logs; bark included 130 × 90 × 50	10.0
4	Torrefied willow briquettes	Rothamsted Research (produced by ECN and C.F. Nielsen, Denmark)	Circular briquettes 20 × 50 (length × diam.)	7.6
5	Olive stone	Arigna Fuels, Arigna, Ireland	Briquettes, stone shaped 50 × 35 × 25	14.8
6	Torrefied olive stone briquettes	Arigna Fuels, Arigna, Ireland	Briquettes, stone shaped 50 × 35 × 25	6.4

ar: as received.

The present work explores this further: A fixed grate stove with a single combustion chamber has been used with two wood fuels and one industry waste (olive stone), as well as their torrefied forms in a comparative study. Particulate and gaseous emissions were measured over three continuous combustion cycles, the first cycle being a cold start, the second two reload cycles. The resultant emissions were monitored and compared between the original and torrefied forms; this was to understand the impacts of torrefaction on combustion phases- ignition, flaming and smouldering. Some sampling was made once the flue gases were diluted, this was to obtain a particle size distribution for particulate emissions from different fuels in diluted circumstances. Fuels have been characterised by a number of approaches including pyrolysis-GC-MS to help understand and interpret the observed emission profiles.

2. Material and methods

2.1. Fuels studied

Six fuels were studied, three of which are in the torrefied form, and details are given in Table 1, together with the shape and dimensions of the fuels. Before chemical analysis the biomass was shredded to a size of < 1 mm, and milled using a Retsch cryogenic mill to between 10 and 100 µm. Proximate analysis was undertaken in accordance with BS EN 144774-3 for moisture, BS EN 15148 for volatile matter, BS EN 14775 for ash, the residual percentage being fixed carbon (FC). Ultimate analysis (CHNS) was carried out on a CE Instruments Flash EA1112, the oxygen content was calculated by difference.

All torrefied fuels were manufactured by external suppliers. The torrefaction processes are: (a) torrefied spruce (by Andritz AG), heated at a temperature of 260 °C for 30–40 min, (b) torrefied willow (ECN), heated at a temperature of 250–260 °C for 90 min, and (c) olive residue was torrefied by heating at 280 °C for 100 min, but the final fuel briquette was approximately a 50:50 blend (by mass) with untreated olive stone to improve the binding/handling properties of the briquettes.

2.2. Combustion tests

All tests were carried out using a fixed bed stove (Waterford and Stanley Oisin); this is a multi-fuel stove commonly used in domestic heating applications and previously described by us [14,29]. The combustion chamber has dimensions of 250 × 270 × 190 mm (height × width × depth), a stated thermal efficiency of 79% and non-boiler thermal output of 5.7 kW. The primary air flow was controlled so there was 150% excess air as recommended by the manufacturer. The flue gases pass through an insulated stainless-steel flue stack with internal diameter of 125 mm, the flue gases were drawn into an extraction system which creates a static pressure of 12 Pa in accordance with BS12340. The stove was placed on an electronic balance to measure the

mass burning rate and the total mass consumption. The arrangement is in accordance with BS EN 13240.

Samples of gases and particulates were taken through ports in the flue stack 1430 mm from the top of the stove. The gases are drawn through a stainless steel probe heated at 180 °C. Gaseous emissions were measured using a GASMET 4040 FTIR exhaust gas analyser. NOx was not determined by the FTIR instrument because of optical interference problems; rather NOx was measured using a Testo Model 340 analyser. Samples for particulate measurements were taken through the same port but via a separate heated line and the gases were passed through a heated (70 °C) filter block in which were mounted Munkter 50 mm diameter micro-quartz filter papers. Two filter papers were placed in the filter block, the first captures the majority of the sample whilst the second acts as a backing filter; the backing filter is usually used qualitatively to determine colour changes in the deposited material. The system is maintained at 70 °C to prevent condensation of any organic matter as in accordance with BS 3841-3: 1994. Sampling takes place for a known time period, the length being dependent on the combustion phase and fuel type.

A Dekati PM₁₀ impactor is used to measure the particle size distribution. These samples were taken from within the dilution tunnel approximately 4500 mm from the top of the stove. This system permits separation into size ranges ≥ 10 µm, 10–2.5 µm, 2.5–1 µm and ≤ 1 µm and operates in accordance with ISO23210. Flue gas flow rates were measured using a Wöhler DC100 unit for pressure measurements coupled with an S-type pitot tube, in accordance with BS EN ISO 16911-1.

Each fuel was loaded into the stove in a similar way, however because some of the fuels are logs and others briquettes it was difficult to obtain consistency in the geometrical distribution because of the different shape and size. Between 0.7 and 0.9 kg of fuel was loaded in each batch and pieces of kerosene-based solid firelighter (Zip High Performance) with a mass of 50 g were used to ignite the first batch of fuel from a cold start- i.e. room temperature. As in the work of Mitchell et al. [14], the emissions during the start-up phase were excluded in emission factor calculations due to the effect of the firelighters.

Gaseous emission factors in kg/GJ were calculated from the average emissions (mg/m³) across a specific time window and the specific dry flue gas volume (SDFGV) which was calculated from the ultimate analyses data [29]. This calculation is based on BS EN 12952-15:2003. Particulate Matter emission factors were calculated using the same method so as to incorporate effects of different batch loads and variations in fuel properties. Emission factors were calculated across a specific combustion cycle where the total mass of fuel consumed is measured.

Py GC-MS of the fuel samples were obtained using a CDS Pyroprobe Model 5000 interfaced to a Shimadzu GC-MS, Model QP2010E. The Pyroprobe sample heating rate was set at 20 °C/ms reaching a final temperature of 550 °C with a hold time of 60 s.

The GC/MS operating conditions were: start at 40 °C hold for 2 min,

heated at 10 °C/min to 180 °C then held for 2 min, then heated at 8 °C to 280 °C then held for 10 min. The carrier gas was helium and a RTX-1701 fused silica column is 60 m in length with 0.32 mm diameter (0.25 µm thickness) with a column flow is 1.34 mL/min. The ion source temperature was 260 °C and the Interface temperature 280 °C.

2.3. Fuel properties

The physical shapes of the fuels have been described in Table 1 and they influence the combustion behaviour. It should be noted that whilst the shape and size of the torrefied fuels and olive are uniform since they are briquetted, the spruce and willow logs show greater variations in dimensions. However the mass of fuel loaded into the stove was kept the same as far as possible. It should be noted also that the briquettes differed in their degree of hardness, some readily disintegrated during combustion which is an important practical factor determining the combustion rate, and so the durability of the fuels is an important consideration in the resulting emissions. The torrefied willow briquettes are the least durable and rapidly break up during combustion. In fact, as soon as they begin to flame they start to disintegrate. The olive and torrefied olive briquettes may be described as being of medium durability, they disintegrate at the end of flaming combustion as the glowing char combustion phase begins. The logs and the torrefied spruce briquettes are described as ‘durable’ in comparison, since they maintain their shape throughout combustion. However, when more fuel is placed on top of them the weight of the new fuel begins to break their structure.

The proximate and ultimate analysis results for each fuel are given in Table 2. This data represents typical analysis of the fuels. Some variation is expected due to the heterogeneous nature of the fuel, and hence there will be variation in the analysis of the actual fuel that is fired. In addition, in these studies bark is included which adds another factor in the heterogeneity, and sampling errors that may result during the analysis. Thus, whilst the expected analytical measurement errors are those specified in the standard analytical methods used ($\pm 0.2\%$), the actual errors here are greater: particularly in relation to the moisture content in the proximate analyses, and the volatile content of the torrefied olive because it is a blend with untorrefied fuel and also appears non-uniform in degree of torrefaction. These errors are shown in Table 2.

The degree of torrefaction varied from fuel to fuel because the torrefaction conditions differed slightly. Li et al. [30] define degree of torrefaction as the % loss of volatile matter on a dry basis compared with the parent biomass. Using this definition, we find the degrees of torrefaction as 7.8% (torrefied spruce), 11.0% (torrefied willow) and 20.7% (torrefied olive), respectively. Note that these represent estimations since we do not have exactly the same parent biomass for the

Table 2
Proximate and ultimate analyses of the raw and torrefied (T) fuels studied,

Fuel	Spruce	T. spruce	Willow	T. willow	Olive	T. olive
Volatile matter (%db)	77	71	82	73	82	65
Ash (%db)	0.4	1.0	1.0	2.8	1.2	4.9
FC (%db)	22.6	28	17	24	17	30
Moisture (%ar)	18	4.6	10	7.6	14.8	6.4
C (%daf)	51	58	49	56	56	70
H (%daf)	6.1	6.1	6.3	5.2	5.2	3.7
N (%daf)	0.27	0.49	0.56	0.64	0.50	0.56
S (%daf)	0.04	0.04	0.04	0.06	0.10	0.20
O (%daf)	42	35	44	38	38	27
K ppm, db	840	1280	2660	3650	1600	1900
GCV (MJ/kg db)	19.70	23.03	18.98	21.25	21.51	25.34

ar: as received; db: dry basis; daf: dry ash free. O calculated by difference. The relative percent error is estimated as better than $\pm 4\%$ except in the case of the olive and torrefied olive samples which are more variable and the relative percent error is better than $\pm 10\%$.

torrefied material. Also, this is a pseudo-extent of torrefaction for the olive, since this briquette is made of a blend of olive and torrefied olive.

Data statement: All data is provided in the body of the text and in the Supplementary material.

3. Results and discussion

3.1. Measurement of burning rates

Previous research has identified several stages of combustion [14,23], but because there is no consistent method for defining all the phases of combustion it is simpler to define the three principal phases, ignition, flaming and smouldering. Here we use a definition that when the burning rate is > 0.85 kg/h it is defined as ‘flaming’, and when the burning rate is consistently lower than 0.85 kg/h but is > 0.3 kg/h it is defined to be ‘smouldering’. The combustion end point was defined when a mass of 200 g remained (of the order of 25% of the starting mass remained).

Fig.1 shows the variation of the burning rates with time for the olive and torrefied olive fuels, the larger spikes are the flaming combustion phases for the ignition batch and the three reloaded batches (reloading is represented by the arrows). The olive fuel has a higher VM content and a higher peak burning rate than the torrefied olive fuel. Similar plots for the willow and spruce fuels are given in Figs. S1 and S2 in the Supplementary material.

Of particular note in Fig. 1 is the sharp peak in burning rate when the olive briquettes are loaded (average peak width 8 ± 3 min) compared to the much broader peak in burning rate when the torrefied olive briquettes are loaded (average peak width 17 ± 4 min). This has implications for the accurate measurements of burning rates and the emissions data, which is discussed later.

Table 3 gives the average flaming and smouldering burning rates for all the fuels. The VM contents in torrefied willow and spruce are very similar, yet the burning rates during flaming combustion are very different. This is a result of the physical structure of the fuel, namely the durability and ease of disintegration: the willow briquettes break apart easily during combustion, thus there is a greater surface area available for combustion compared to the spruce briquettes. Consequently the flue gas temperature is highest for the willow briquettes.

The comparison pairs, willow, torrefied willow, and olive, torrefied olive follow the trend that the smouldering burning rate increases with the increased fixed carbon content (FC) given in Table 2, as previously demonstrated [14]. The smouldering burning rates for spruce and torrefied spruce are rather similar because torrefied spruce retains its shape for the duration of most of the combustion; in addition the torrefied spruce has the lowest extent of torrefaction. This is not the case for the willow, and when a briquette disintegrates the burning rate is enhanced, and flue gas temperature increases as a result.

3.2. Measurement of gaseous emission factors

The principal carbon-containing gaseous emissions are carbon dioxide (CO₂), carbon monoxide (CO) and methane (CH₄). Fig. 2 shows the results for CO₂ and CO emissions from torrefied willow over the ignition and three subsequent combustion cycles; these are presented on a dry basis at 13% oxygen, normal room temperature (20 °C) and pressure. Similar plots for the other fuels are given in the Supplementary material (Figs. S3–S7). The first cycle involves ignition and the initial heating up of the fuel bed and stove, but here attention is mainly directed to the subsequent cycles, indicated by the arrows. Here the fuel is manually loaded by opening the stove door but additionally there is an inflow of air. This has consequences in the definition of the start of the flaming phase and thus on the associated emission factors. Initially the wood undergoes devolatilisation and the resultant gaseous volatiles are rapidly oxidised to CO, followed by the slower conversion to CO₂. Thus the CO profile consists of an initial sharp peak (at $t = 47, 84$, and

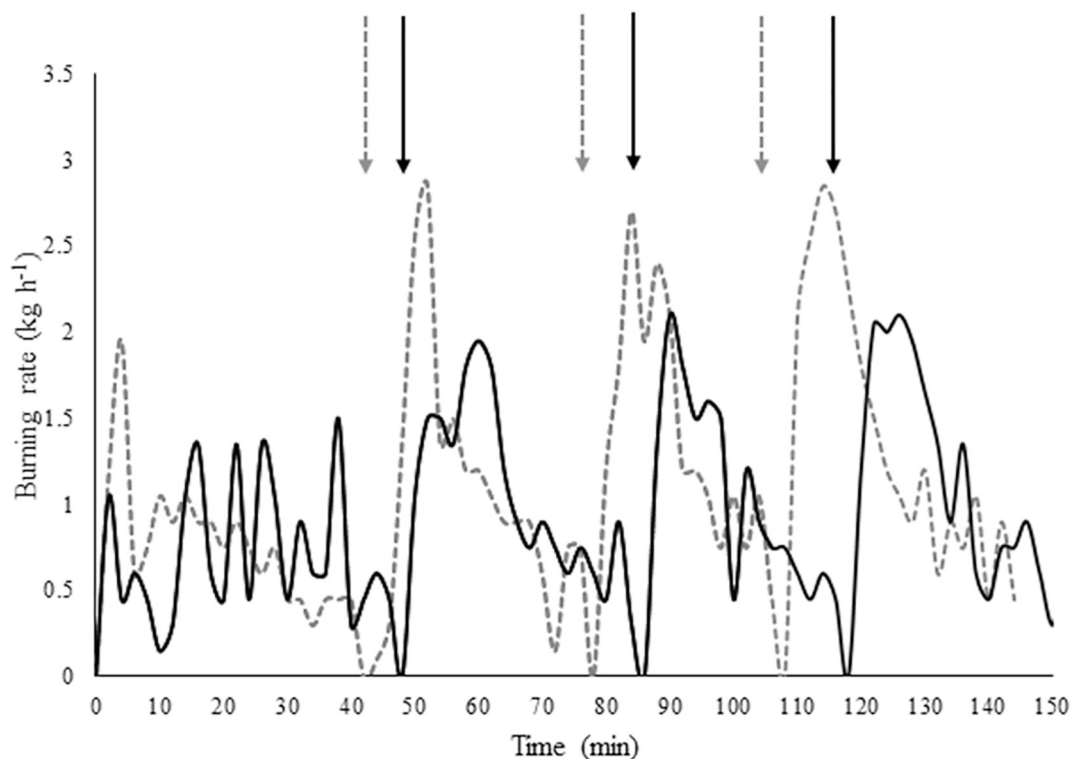
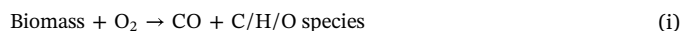


Fig. 1. Variation of burning rates with time for the olive waste (dashed line) and torrefied olive waste (solid line). The points of fuel reloading are shown for both by vertical arrows.

116 min) due to the slow mixing with oxygen which rapidly declines to the minimum level ($t = 61, 96,$ and 129 min) during the flaming phase, as shown in Fig. 2; but once the smouldering phase commences the CO emission slowly increases resulting from the heterogeneous combustion of the char formed.

Table 4 gives the emission factors for the carbon-containing species, CO_2 , CO and CH_4 , for all the fuels studied; these values represent the average over a whole cycle. It is seen that the CO_2 emission factors are higher for the torrefied fuels, due to the higher fixed carbon (FC) content of the fuels as shown in Table 2. The CO emission factors are the same for most fuels but the raw spruce has a slightly higher value; this may result from the higher moisture content which reduces the combustion temperature. Torrefied fuels have a broader peak in the burning rate during flaming combustion, as shown, for example, for olive in Fig. 1. This could be due to two factors: firstly, the rate of devolatilisation is considerably reduced in torrefied fuels (which are essentially already partially devolatilised) [31], and secondly, the nature of the volatiles differs. This is discussed later in relation to the Pyrolysis-GC-MS results.

The emission factors of CH_4 are higher for the spruce, torrefied spruce and willow, compared to the other fuels. Profiles are given in S8–S10 in Supplementary material. These are largely dictated by the C/H content of the fuels since the methane is formed by decomposition and gasification of the volatiles [32] as given in the reactions below. Effectively the concentrations of CO and CH_4 are in partial equilibrium with one another.



The emission of NOx is largely dictated by the fuel-nitrogen content in the biomass since the temperatures and reaction times in the multi-fuel unit preclude the formation of thermal-NO. The reaction conditions also only permit formation of very small amounts of N_2O and NO_2 , although the latter may be formed later from NO in the cooled flame gases or sampling lines. The formation of NO from a typical experiment using the olive and torrefied olive is shown in Fig. 3. Further profiles

Table 3

Burning rates for flaming and smouldering combustion, average flue temperatures (1.43 m above the combustion zone) and the percentage of the initial batch load mass when the combustion phase changes.

Fuel	Burning rate, kg/h, flue gas temperature in parenthesis				
	Flaming		Smouldering		Average per load
	Average	% of initial mass	Average	% of initial mass	
Spruce	1.55 (225 °C)	38 ± 5	0.67 (175 °C)	15 ± 3	1.27
T. spruce	1.19 (240 °C)	35 ± 3	0.65 (180 °C)	12 ± 2	0.94
Willow	1.86 (320 °C)	27 ± 3	0.72 (255 °C)	14 ± 2	1.41
T. willow	2.85 (395 °C)	21 ± 3	0.73 (325 °C)	12 ± 2	2.30
Olive	1.41 (370 °C)	40 ± 6	0.51 (300 °C)	16 ± 2	1.24
T. olive	1.21(380 °C)	43 ± 2	0.62 (300 °C)	20 ± 4	1.02

Note: The weights of the firefighters are excluded.

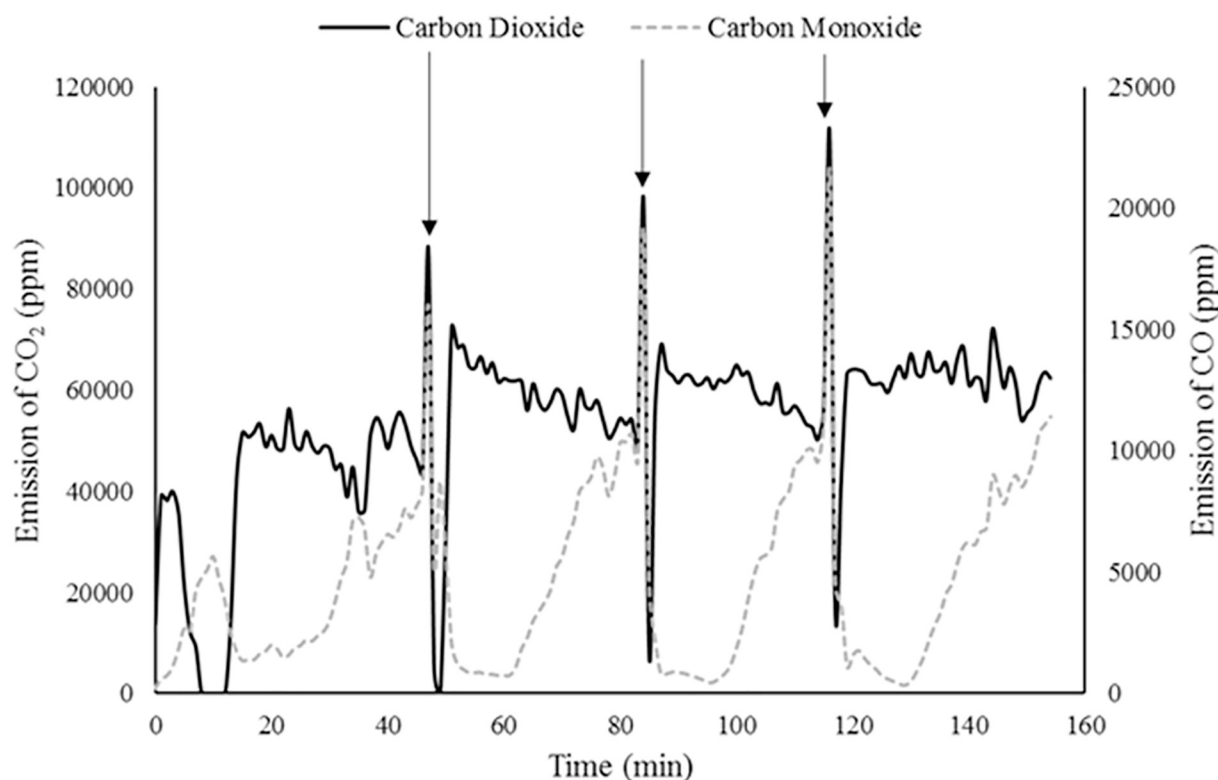


Fig. 2. Emission of CO₂ (solid line) and CO (dashed line) over combustion period for torrefied willow. The arrow indicates the point of fuel reloading.

are given in the Supplementary material, Figs. S11 and S12. The emission of NO_x from olive is different to that of the torrefied fuel. The peak of NO release behaves differently in both fuels, firstly in the difference in the magnitude of the NO_x emission (olive peaks are 371, 320, 317 mg m⁻³ and torrefied olive peaks are 258, 285 and 279 mg m⁻³), but also there is a difference in the shape of the curve. The NO_x emission from the torrefied fuel persists longer into the smouldering phase.

Table 5 shows the emission factors for NO_x for the fuels studied and it is clear that the emissions are primarily NO. The linear relationship of the emission factors to the fuel-N contents is seen in Fig. 4 for the (non-torrefied) woods and the olive and this is consistent with previous work [14,33,34]. It is seen that that is an approximate linear relationship with the fuel-N content for the raw materials. There is also a small predicted emission in the case of zero fuel-N and this would correspond to the small contribution of thermal-NO.

The behaviour of the torrefied fuels is different. It is seen from Table 2 that the N-content increases during torrefaction on a weight basis. In spite of this, the NO_x emissions are lower on a thermal and mass basis for the torrefied compared to the non-torrefied analogues as shown in Table 5. There is some evidence, at least in the case of olive [15], that torrefied fuels contain char-like material and thus the atomic

N could be more tightly bound to the char matrix. In that case it would be released during combustion as N₂ rather than NO due to the greater reducing nature of the char. This would apply during both the flaming and smouldering phases. This theory is supported by N-analyses of the residues after combustion, which are also given in Table 5. Analyses are for the bottom ashes which had been burned to 80% burnout (i.e. 20% of material remaining). It is clear that a similar fraction of fuel-N is evolving during combustion, irrespective of whether the material has been torrefied or not.

Although here the torrefied fuels are not exactly from the same material as the raw fuels, the effect of energy intensification is interesting. It can be concluded that fuel nitrogen compounds are not preferentially lost during the torrefaction process and so torrefaction is not beneficial in this application in terms of N-content. However, in terms of NO_x emissions resulting from combustion, there is some compensation for the higher wt% N in the torrefied fuels, since NO_x emissions are lower on a per GJ basis in the energy densified fuels.

3.3. Particulate emissions (PM)

There is a particular interest in particulate emissions because of the potentially severe health effects from very small particles, climate

Table 4

Comparison of emission factors and gaseous emission concentrations, averaged over a whole cycle, the margin of error is shown in the parenthesis for a 95% confidence interval.

Fuel	g/GJ			g/m ³ at 13% O ₂		
	CO ₂	CO	CH ₄	CO ₂	CO	CH ₄
Spruce	65 (± 20)	5.8 (± 0.44)	0.37	115 (± 32)	9.1 (± 1.2)	0.56
T. spruce	90 (± 5.2)	3.2 (± 0.1)	0.18	145 (± 10)	6.0 (± 0.32)	0.47
Willow	67 (± 16)	4.2 (± 0.24)	0.18	110 (± 33)	7.0 (± 0.69)	0.34
T. willow	78 (± 16)	4.2 (± 0.53)	0.04	120 (± 32)	6.9 (± 1.4)	0.10
Olive	73 (± 10)	4.0 (± 0.25)	0.05	110 (± 28)	6.6 (± 0.71)	0.18
T. olive	74 (± 5)	4.2 (± 0.44)	0.05	98 (± 17)	6.0 (± 1.2)	0.13

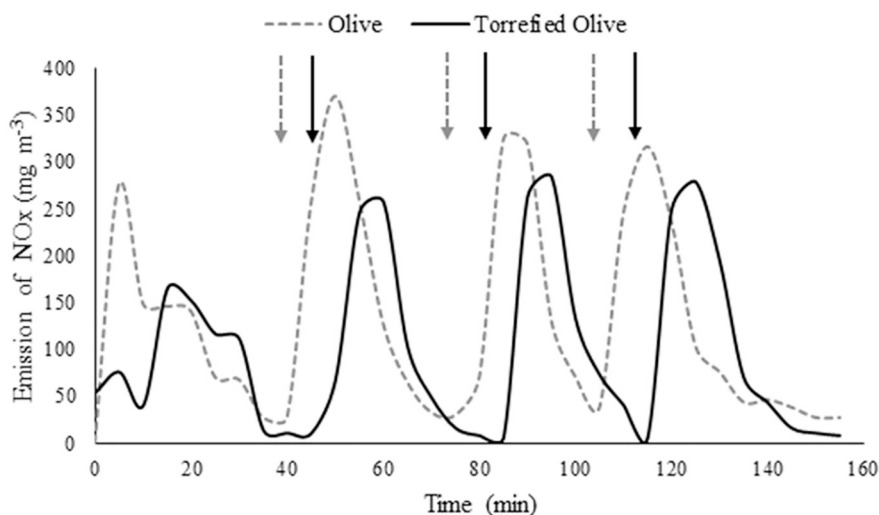


Fig. 3. Comparison of NOx emissions from the olive (dashed line) and torrefied olive (solid line).

Table 5

Emission factors for NOx over the whole combustion cycle,^a and nitrogen contents remaining in the unburned bottom ash/char. Margins of errors are given.

Fuel	NOx emission factors		Fuel-N content	Residual char-N
	g/GJ	g/kg	wt% daf	%
Spruce	50 (± 12)	0.388	0.27	18 ± 0.06
T. spruce	45 (± 5.1)	1.04	0.49	17 ± 0.09
Willow	135 (± 8.5)	2.56	0.56	7 ± 0.12
T. willow	90 (± 20)	1.91	0.64	8 ± ± 0.10
Olive	75 (± 24)	1.61	0.50	10 ± 0.10
T. olive	60 (± 17)	1.52	0.56	10 ± 0.04

^a Each cycle burns until ~200 g of fuel remains.

(radiative forcing) effects as well as the aesthetic expectations of consumers. The experimental Emission Factors for PM are summarised in Table 6 where the sub-micron content is also shown. For the two woods the amount of smoke produced is a function of the volatile content, as

Table 6

Table of VM and atomic C/H ratios of the fuel, EF PM (total averaged over the complete cycle) and % sub-micron (PM₁) content.

Fuel	VM (% db)	Atomic C/H	EF, PM (total) g/kg	PM ₁ (%)
Spruce	77	0.70	4.2	97.6
T. spruce	71	0.79	2.2	98.6
Willow	82	0.65	6.4	96.5
T. willow	73	0.90	4.9	96.6
Olive	82	0.90	6.7	99.0
T. olive (50/50 blend)	65	1.56	4.6	98.3

previously shown for this stove [14] and whether the fuels have been torrefied; this last factor is the major factor in determining the emission of smoke.

There are experimental difficulties in making accurate estimates of the emission factors over a whole combustion cycle for wood because the start and end points are difficult to define. Initially, whether during

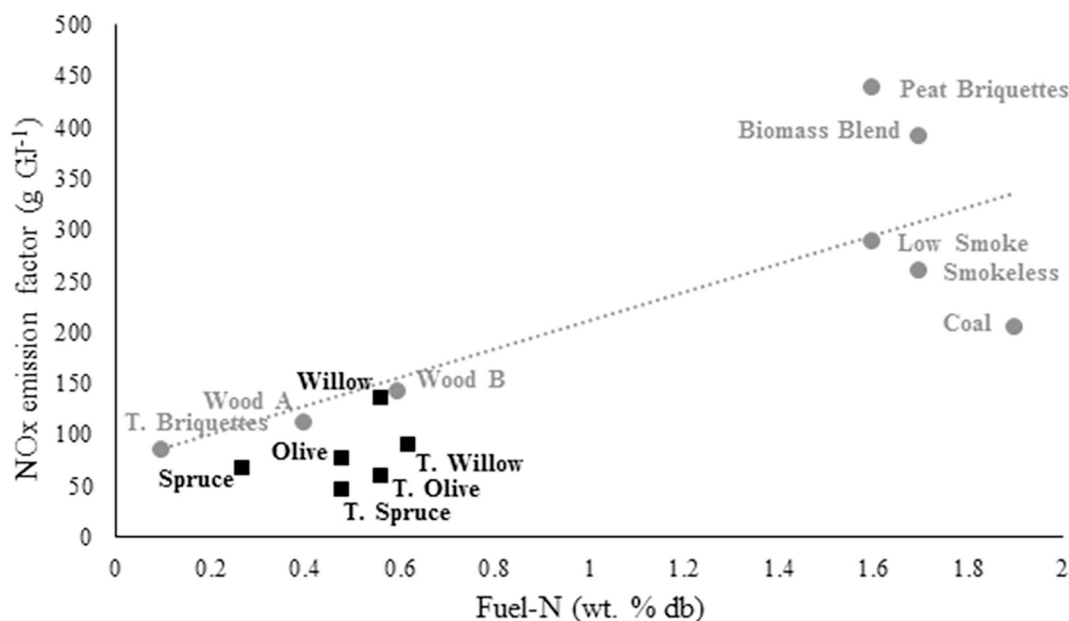


Fig. 4. Emission factors of NOx over the complete combustion cycle as a function of the fuel-nitrogen content. This study, ■: Mitchell et al. [14], ●. The errors are given in Table 5.

the first ignition or the subsequent reloading to the smouldering fuel there is a perturbation of the particulate emission. For the torrefied fuels, characteristics of flaming and smouldering stages differ, which introduces further inherent challenges in making these judgements. Consequently, some large differences in EF are reported between different operators. However, if operator error can be lowered then comparison of EF within a data set becomes more reliable. This is the case in the present study, and it is estimated that the experimental errors within the data set of EF is of the order of $\pm 20\%$. The results generally are in agreement with other studies discussed here.

The results in Table 6 show how torrefaction, that is, increasing the aromaticity (C/H) leads to a reduction in the EF for the particulate matter. The PM is significantly reduced in the case of the torrefaction of spruce, which is consistent with the result of Mitchell et al. [14]. The reduction on torrefaction is less for the faster burning torrefied willow; raw olive stone has the highest particulate emission and the torrefied counterpart has a significantly lower particulate emission.

The effect of moisture content in the untreated woods studied here is not considered to be significant in terms of emission of particulate matter over the range studied since our previous study [29] indicates that the emission of particulate matter for similar woods does not vary significantly over the range of 8 to 22 wt% moisture content. In this study the results for only two torrefied woods were obtained which are insufficient to make a definitive conclusion. But the indications are that these fuels behave in the same way to the woods studied previously.

3.4. Pyrolysis-GC-MS results

A number of studies have been made of the effect of torrefaction on wood and on the chemical composition and physical properties of the torrefied fuel produced [5–7,35,36]. However, there are limited studies published on the Py-GC-MS of torrefied fuels [27,28] and no studies in which the fuels are also used in a real world combustor. Understanding the pyrolysis fingerprint is important since these components contribute to the soot-forming reaction pathways, and some are more sooting than others, as shown in [26]. Here Py-GC-MS studies were made of the fuels listed in Table 1 and the chromatographs are given in Figs. S13–S15 in the Supplementary material.

The main peaks were identified by reference to the NIST mass spectral database library and also existing literature [37–39]. For this particular GC column and conditions, the majority of the decomposition products detected are from the lignin components, which make up of approximately 50–60% of the peak area (calculated as the sum of the areas of identified components). It should be noted, that in the case of the raw olive fuel, there was a broad band of late eluting components (see Fig. S15), typical of fatty acids, but these were not resolved into individual components and so are not included in the total peak areas. Furthermore, it was found that the torrefied olive fuel was non-uniform, and contained a mix of lightly and heavily torrefied material.

Fig. 5 compares the total peak areas for decomposition products from pyrolysis of raw and torrefied fuels. Fig. 5(a) shows the carbohydrate decomposition products (identities are given in Figs. S13–S15), which are seen to increase in the torrefied woody fuels, but decrease markedly in the olive fuel. In the latter case, this is thought to be because of “over torrefying” and points to a need for further optimisation of the production of this fuel. In the case of the woody biomass, this is surprising since it is expected that the torrefaction process, which thermally-degrades hemicellulose, will decrease the carbohydrate components in the volatiles. Further analysis of the data indicates that the increase is mainly the result in an increase in the levoglucosan in the decomposition products of the torrefied woods. Such an increase has been reported previously for other types of biomass [40,41], and a proposed mechanism involves the elimination of hemicellulose-cellulose interactions, and a promotion of cellulose-lignin interactions, during pyrolysis [42].

Fig. 5(b) compares the total peak areas (identities are given in Figs.

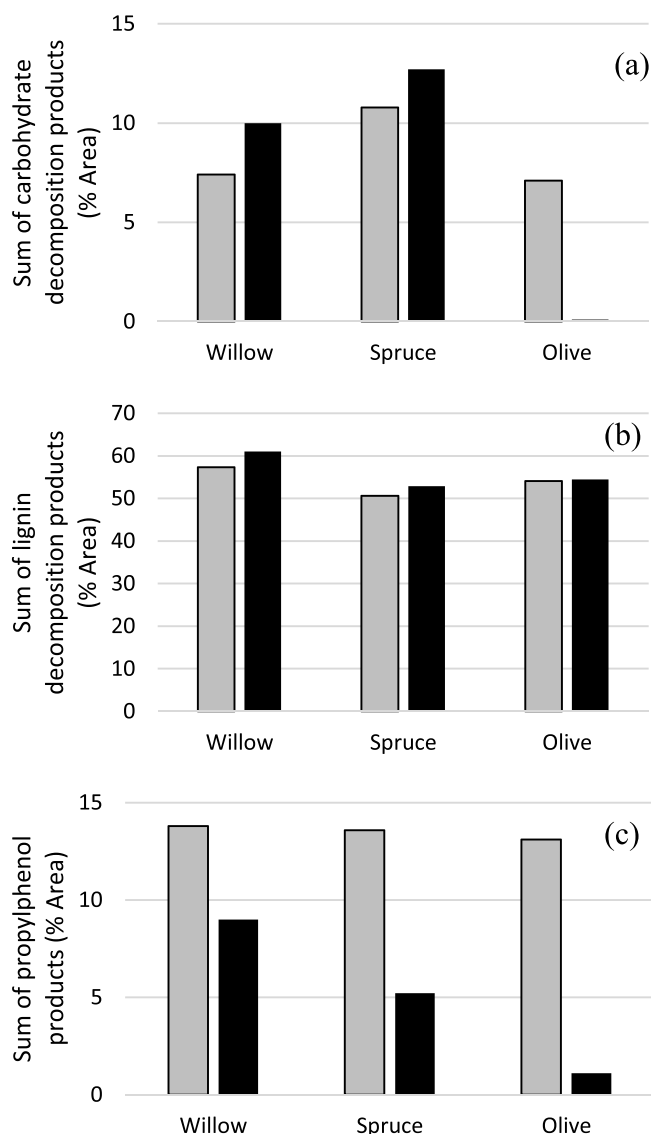


Fig. 5. Sum of peak area % in the pyrolysis-GC-MS of the different fuels. (a) Carbohydrate decomposition products; (b) lignin decomposition products; (c) propylphenol products. Grey – raw biomass; black – torrefied biomass.

S13–S15) for decomposition products from pyrolysis of lignin in raw and torrefied fuels. Here it is seen that there is a very small increase in the total products after torrefaction.

All the pyrolysis components will contribute to soot forming reactions in the combustion system, although some to a greater extent than others, as shown in [26]. It is particularly interesting to examine the propylphenol products from lignin decomposition, since these were found to have the highest sooting tendencies of the compounds studied in [26]. This comparison is made in Fig. 5(c), where the propylphenols detected are eugenol, methoxyeugenol, and homovanillyl alcohol which make up more than a quarter of all the detected lignin decomposition products. It is clearly demonstrated that, after torrefaction, these types of compounds decrease in concentration in the volatiles. This can go part-way to explain the decreased sooting tendencies of torrefied fuels compared to non-torrefied counterparts, presented in Table 6. For Spruce, the decrease in EF_{PM} (by a factor of 1.9) is consistent with the results obtained by Mitchell et al. [14] for briquettes manufactured by Andritz.

Olive-based fuels also have high fatty-acid contents which will also contribute to the soot formation routes, and which decrease markedly

after torrefaction (Fig. S15). In fact, the concentration of fats and fatty acids in the decomposition products (all fuels), were seen to decrease by 50–60% after torrefaction and this will clearly be another causative factor in the reduced particle emissions from the torrefied fuels.

3.5. General features of combustion

The fuels studied are diverse in composition: there are two woods, one with a high moisture content, and an olive stone briquette, together with their torrefied equivalents. The size and shape of the fuel is an influential factor on the combustion of biomass which is not a property of the fuel but of the fuel preparation.

The process of torrefaction, which is a mild pyrolysis process, has been well studied and results in the loss of almost all the hemicellulose, up to 75% of the cellulose (depending on conditions) and a few % of the lignin, resulting in a greater aromaticity as shown by the increase in the atomic C/H ratio on torrefaction. Moisture is also reduced and because of the processing, the product is usually more consistent. There have been extensive studies of the chemical changes taking place during torrefaction and in some cases this includes changes in S and N concentrations [6,7,31,32].

Less is known about the combustion mechanism of torrefied fuels in domestic sized stoves, most experimental combustion studies have been made using pulverised fuel combustion e.g. [30].

A mechanism has been proposed for smoke formation from the combustion of wood [14,26,43,44], whereby pyrolysis products undergo thermal cracking and rearrangement and participate in two main soot-forming routes. Essentially this suggests that the cellulose products can produce acetylene and other building bricks for the HACA (hydrogen abstraction, carbon addition) model. In addition, phenols from lignin decomposition can participate in the route to build polyaromatic hydrocarbons via cyclopentadiene (CPD). Some lignin products, particularly propylphenols, participate in both HACA and CPD routes. In parallel to this, lignin would decompose giving polyphenols which would grow more easily to produce aromatic soot. This model would explain the reduction of particulate soot during the combustion of torrefied fuels: the reduction of cellulose and propylphenols during torrefaction process leads to the formation of a 'less smoking (smokeless) fuel'.

NO_x is typically the result of the fuel nitrogen content especially in domestic stoves. Comparing the emissions of the original fuels to their torrefied forms, all of the fuels show that torrefaction has little impact (or a slight improvement) on the NO_x emissions even though there is a change in the fuel composition. Because these are presented as emission factors the mass increase of nitrogen in the torrefied fuels is counteracted by the energy densification. However, for non-torrefied fuels there is still a relationship between fuel-N and NO_x; NO_x is linearly proportional to the fuel nitrogen content, as observed in other publications [14].

The behaviour of torrefied fuel-N raises questions about the chemical reactions that occur. Normally the fuel-N compounds decompose into volatile-N compounds and char-N. The volatile-N compounds would be involved with the flaming combustion and decompose into HCN and in turn be oxidised in part to NO. The char-N compounds would be involved in the smouldering combustion and would form some HCN/NO product and some N₂. It seems that in torrefied fuels the N-content is trapped into a refractory C-matrix which on combustion tends to form N₂ rather than HCN/NO.

An important factor is the combustion behaviour of the char produced during the flaming process. Only a limited number of studies have been made, but they seem to show that chars produced in the torrefaction process, burn more slowly [45], although the potassium content may be important [45,46]. Products made by hydrothermal processes are not significantly different either in terms of intrinsic reactivity [47]. The major factor determining overall reactivity of a fuel is both the intrinsic reactivity and the surface area exposed to the oxygen

in the air. This issue demonstrated by this work is that torrefied fuels have to be compressed into the form of briquettes and it is the ease of disintegration during the flaming phase that determines their overall combustion rate.

4. Conclusions

1. A comparative combustion study was conducted for two woods and a waste, olive stone, and their equivalent torrefied forms. The fuels were burnt on a batch basis in a fixed bed domestic stove with no secondary combustion in order to determine the initial emissions. The gaseous emissions (CO₂, CO, CH₄, NO_x) follow conventional combustion cycles for unprocessed fuels. The torrefied fuels have a slower burning rate and the flaming phase lasts longer, reducing emissions of CO and CH₄.
2. The torrefaction temperature and physical structure have a significant effect on the combustion behaviour of the torrefied fuel.
3. The particulate matter emitted is reduced by torrefaction and this could be the result of three different effects: pre-treatment and lignocellulosic degradation, the physical structure of the briquette and to a lesser degree the influence of the moisture content.
4. NO_x emissions from torrefied fuels are reduced on a thermal basis suggesting a different mechanism to that found in raw unprocessed fuels.

Overall the use of torrefied fuels is encouraged due to its vast improvements across a range of pollutants to improve air quality and greenhouse gas effects.

Declaration of competing interest

The authors declare that they have no known competing financial interests or personal relationships that could have appeared to influence the work reported in this paper.

Acknowledgements

We wish to thank EPSRC for support via the Centre for Doctorial Training (Grant number EP/L014912/1) and the Supergen Bioenergy Hub (EP/J017302/1). We also would like to acknowledge useful discussions with Dr. P.E. Mason, Dr. E.J.S. Mitchell and Mr. A Price-Allison. We also thank Professor D Spracklen (Leeds University), Dr. P Johnson (Arigna Fuels), Dr. I Shield (Rothamsted Research) for providing fuel samples.

Appendix A. Supplementary data

Supplementary data to this article can be found online at <https://doi.org/10.1016/j.fuproc.2019.106266>.

References

- [1] J.P. Bourgeois, J. Doat, H. Egneus, A. Ellegard (Eds.), *Bioenergy 84, Proceedings of Conference 15–21 June 1984, Goteborg, Sweden. Volume III. Biomass Conversion*, Elsevier Applied Science Publishers, Barking, UK, 1985, pp. 153–159.
- [2] E.S. Lipinsky, J.R. Arcate, T.B. Reed, Enhanced wood fuels via torrefaction, 223rd ACS National Meeting, Orlando, Fuel Chemistry Division Preprints 47 (1) (2002) 408.
- [3] P.C.A. Bergman, A.R. Boersma, R.W.R. Zwart, J.H.A. Kiel, Torrefaction for Biomass Co-firing in Existing Coal-fired Power Stations: "Biocoal". ECN Report. Renewable Energy in the Netherlands, ECN-C-05-013 (2005).
- [4] J.M. Jones, T.G. Bridgeman, L.I. Darvell, B. Gudka, A. Saddawi, A. William, Combustion properties of torrefied willow compared with bituminous coals, *Fuel Proc. Technol.* 101 (2012) 1–9.
- [5] R.H.H. Ibrahim, L.I. Darvell, J.M. Jones, A. Williams, Physicochemical characterisation of a solid torrefied biomass, *J. Anal. Appl. Pyrol.* 103 (2013) 21–30.
- [6] T. Li, M. Geier, L. Wang, X. Ku, B.M. Güell, T. Lovås, C.R. Shaddix, Effect of torrefaction on physical properties and conversion behavior of high heating rate char of forest residue, *Energy Fuel* 29 (2015) 177–184.
- [7] Final Report Summary - SECTOR (Production of Solid Sustainable Energy Carriers

- from Biomass by Means of Torrefaction) CORDIS FP7-ENERGY, <https://cordis.europa.eu/project/rcn/101152/reporting/en>.
- [8] D. Braken, Woody Biomass for Power and Heat Impacts on the Global Climate Environment, The Royal Institute of International Affairs, Chatham House, London, 2017.
 - [9] J.D. Stermann, L. Siegel, J.N. Rooney-Varga, Does replacing coal with wood lower CO₂ emissions? Dynamic lifecycle analysis of wood bioenergy, *Environ. Res. Lett.* 13 (2018) 015007.
 - [10] M. Röder, C. Whittaker, P. Thornley, How certain are greenhouse gas reductions from bioenergy? Life cycle assessment and uncertainty analysis of wood pellet-to-electricity supply chains from forest residues, *Biomass Bioenergy* 79 (2015) 50–63.
 - [11] A. Welfle, P. Gilbert, P. Thornley, A. Stephenson, Generating low-carbon heat from biomass: life cycle assessment of bioenergy scenarios, *J. Clean. Prod.* 149 (2017) 448–460.
 - [12] P. McNamee, P.W.R. Adams, M.C. McManus, B. Dooley, L.I. Darvell, A. Williams, J.M. Jones, An assessment of the torrefaction of North American pine and life cycle greenhouse gas emissions, *Energ. Convers. Manage.* 113 (2016) 177–188.
 - [13] J-B. Michel, M. McCormick, Experimental investigation of continuous torrefaction conditions of biomass residues for the subsequent use of torrefied pellets in domestic and district heating systems, 10th European Conference on Industrial Furnaces and Boilers, 2015 Gaia (Porto) Portugal.
 - [14] E.J.S. Mitchell, A.R. Lea-Langton, J.M. Jones, A. Williams, P. Layden, R. Johnson, The impact of fuel properties on the emissions from the combustion of biomass and other solid fuels in a fixed bed domestic stove, *Fuel Proc. Technol.* 142 (2016) 115–123.
 - [15] A. Trubetskaya, J.J. Leahy, E. Yazhenskikh, M. Müller, P. Layden, R. Johnson, K. Stahl, R.F.D. Monaghan, Characterization of woodstove briquettes from torrefied biomass and coal, *Energy* 171 (2019) 853–865.
 - [16] T. Li, L. Wang, X. Ku, B.M. Güell, T. Lovås, C.R. Shaddix, Experimental and modeling study of the effect of torrefaction on the rapid devolatilization of biomass, *Energy Fuel* 29 (2015) 4328–4338.
 - [17] A. Valavanidis, K. Fiotakis, T. Vlachogianni, Airborne particulate matter and human health: toxicological assessment and importance of size and composition of particles for oxidative damage and carcinogenic mechanisms, *J. Environ. Sci. Heal. c* 26 (2008) 339–362.
 - [18] A.K. Bølling, J. Pagels, K.E. Yttri, L. Barregard, G. Sallsten, P.E. Schwarze, C. Boman, Health effects of residential wood smoke particles: the importance of combustion conditions and physicochemical particle properties, *Part. Fibre Toxicol.* 6 (2009) 20.
 - [19] J. Orasche, J. Schnelle-Kreis, C. Schön, H. Hartmann, H. Ruppert, J.M. Artega-Salas, R. Zimmermann, Comparison of emissions from wood combustion. Part 2: impact of combustion conditions on emission factors and characteristics of particle-bound organic species and polycyclic aromatic hydrocarbon (PAH)-related toxicological potential, *Energy Fuel* 27 (2013) 1482–1491.
 - [20] A. Muala, G. Rankin, M. Sehlstedt, J. Unosson, J.A. Bosson, et al., Acute exposure to wood smoke from incomplete combustion - indications of cytotoxicity, *Part Fibre Toxicol* 12 (2015) 33.
 - [21] T. Torvela, J. Tissari, O. Sippula, T. Kaivosoja, J. Leskinen, A. Virén, A. Lähde, J. Jokiniemi, Effect of wood combustion conditions on the morphology of freshly emitted fine particles, *Atmos. Environ.* 87 (2014) 65–76.
 - [22] S. Ozgen, S. Caserini, S. Galante, S. Galante, M. Giugliano, E. Angelilino, et al., Emission factors from small scale appliances burning wood and pellets, *Atmos. Environ.* 94 (2014) 144–153.
 - [23] F. Fachinger, F. Drewnick, R. Giere, S. Borrmann, How the user can influence particulate emissions from residential wood and pellet stoves: emission factors for different fuels and burning conditions, *Atmos. Environ.* 158 (2017) 216–226.
 - [24] H. Lamberg, J. Tissari, J. Jokiniemi, O. Sippula, Fine particle and gaseous emissions from a small-scale boiler fueled by pellets of various raw materials, *Energy and Fuels* 27 (2013) 7044–7053.
 - [25] F.A. Atiku, E.J.S. Mitchell, A.R. Lea-Langton, J.M. Jones, A. Williams, K.D. Bartle, The impact of fuel properties on the composition of soot produced by the combustion of residential solid fuels in a domestic stove, *Fuel Process. Technol.* 151 (2016) 117–125.
 - [26] F.A. Atiku, A.R. Lea-Langton, K.D. Bartle, J.M. Jones, A. Williams, I. Burns, G. Humphries, Some aspects of the mechanism of formation of smoke from the combustion of wood, *Energy and Fuels* 31 (2017) 1935–1944.
 - [27] F.S. Akinrinola, Torrefaction and Combustion Properties of Some Nigerian Biomass, PhD Thesis University of Leeds, UK, 2014.
 - [28] S. Ramos-Carmona, J.F. Pérez, M.R. Pelaez-Samaniego, R. Barrera, M. Garcia-Perez, Effect of torrefaction temperature on properties of patula pine, *Maderas. Ciencia y tecnología* 19 (2017) 39–50.
 - [29] A. Price-Allison, A.R. Lea-Langton, E.J.S. Mitchell, B. Gudka, J.M. Jones, P.E. Mason, A. Williams, Emissions performance of high moisture wood fuels burned in a residential stove, *Fuel* 239 (2019) 1038–1045.
 - [30] J. Li, E. Biagini, W. Yang, L. Tognotti, W. Blasiak, Flame characteristics of pulverized torrefied-biomass combustion with high temperature air, *Combust. Flame* 160 (2013) 2585–2594.
 - [31] A. Saddawi, J.M. Jones, A. Williams, C. Le Coeur, Commodity fuels from biomass through pretreatment and torrefaction: effects of mineral content on torrefied fuel characteristics and quality, *Energy Fuel* 26 (2012) 6466–6474.
 - [32] C.K.W. Ndiema, F.M. Mpendazoe, A. Williams, Emissions of pollutants from a biomass stove, *Energy Convers. Manage.* 39 (1998) 1357–1367.
 - [33] M.M. Roy, K. Corscadden, An experimental study of combustion and emissions of biomass briquettes in a domestic wood stove, *Appl. Energy* 99 (2012) 206–212.
 - [34] P. Sommersacher, T. Brunner, I. Obernberger, Fuel indexes: a novel method for the evaluation of relevant combustion properties of new biomass fuels, *Energy Fuel* 26 (2012) 380–390.
 - [35] J.S. Tumuluru, R.D. Boardman, C.T. Wright, J.R. Hess, Some chemical compositional changes in miscanthus and white oak sawdust samples during torrefaction, *Energies* 5 (2012) 3928–3947.
 - [36] T.K. Shoulaifar, N. DeMartini, S. Willför, A. Pranovich, A.I. Smeds, et al., Impact of torrefaction on the chemical structure of birch wood, *Energy Fuel* 28 (2014) 3863–3872.
 - [37] B.R.T. Simoneit, Biomass burning — a review of organic tracers for smoke from incomplete combustion, *Appl. Geochem.* 17 (2002) 129–162.
 - [38] D.J. Nowakowski, J.M. Jones, Uncatalysed and potassium-catalysed pyrolysis of the cell-wall constituents of biomass and their model compounds, *J. Anal. Appl. Pyrolysis* 83 (2008) 12–25.
 - [39] R. Fahmi, A.V. Bridgwater, L.I. Darvell, J.M. Jones, N. Yates, S. Thain, I.S. Donnison, The effect of alkali metals on combustion and pyrolysis of *Lolium* and *Festuca* grasses, switchgrass and willow, *Fuel* 86 (2007) 1560–1569.
 - [40] Z. Yang, M. Sarkar, A. Kumar, J.S. Tumuluru, R.L. Huhnke, Effects of torrefaction and densification on switchgrass pyrolysis products, *Bioresour. Technol.* 174 (2014) 266–273.
 - [41] A. Zheng, Z. Zhao, S. Chang, Z. Huang, X. Wang, F. He, H. Li, Comparison of the effect of wet and dry torrefaction on chemical structure and pyrolysis behaviour of corncobs, *Bioresour. Technol.* 176 (2014) 15–22.
 - [42] T. Hosoya, H. Kawamoto, S. Saka, Solid/liquid-and vapor-phase interactions between cellulose-and lignin-derived pyrolysis products, *J. Anal. Appl. Pyrolysis* 85 (2009) 237–246.
 - [43] E.M. Fitzpatrick, J.M. Jones, M. Pourkashanian, A.B. Ross, A. Williams, K.D. Bartle, K. Kubica, The mechanism of the formation of soot and other pollutants during the co-firing of coal and pine wood in a fixed-bed combustor, *Fuel* 88 (2009) 2409–2417.
 - [44] T. Zhang, X. Li, X. Qiao, M. Zheng, L. Guo, W. Song, W. Lin, Initial mechanisms for an overall behavior of lignin pyrolysis through large-scale ReaxFF molecular dynamics simulations, *Energy Fuel* 30 (2016) 3140–3150.
 - [45] P. McNamee, L.I. Darvell, J.M. Jones, A. Williams, The combustion characteristics of high-heating-rate chars from untreated and torrefied biomass fuels, *Biomass Bioenergy* 82 (2015) 63–72.
 - [46] T.K. Shoulaifar, N. DeMartini, O. Karlstrom, J. Hemming, M. Hupa, Impact of organically bonded potassium on torrefaction: part 2. Modelling, *Fuel* 168 (2016) 107–115.
 - [47] R.J. Stirling, C.E. Snape, W. Meredith, The impact of hydrothermal carbonisation on the char reactivity of biomass, *Fuel Proc* 177 (2018) 152–158.